Cureus Journal of Engineering
https://doi.org/10.7759/s44388-026-00321-1

Original Article

Development of a Zinc-Based Nanocomposite Embedded in a Silica Matrix and Analysis Using Ultraviolet (UV)-Visible Spectroscopy and Scanning Electron Microscopy

Aakarsh Chaudhary [1] , Asima Imtiyaz [2] , Ajay Singh [3,]

1. *Mechanical Engineering, Sardar Vallabhbhai National Institute of Technology, Surat, IND*
2. *Chemistry, Uttaranchal University, Dehradun, IND*
3. *Nanotechnology and Environmental Chemistry, Uttaranchal University, Dehradun, IND*

Received: January 02, 2026 | Review began: February 12, 2026 | Review ended: September 01, 2026 | Published: October 12, 2026

© **Copyright** 2026
This is an open access article distributed under the terms of the Creative Commons Attribution License CC-BY 4.0., which permits unrestricted use, distribution, and reproduction in any medium, provided the original author and source are credited.

Abstract

Nanotechnology plays a very important role in the development of new composite materials by embedding selective metals into the matrix phase. This paper highlights how zinc nanoparticles can be embedded into the matrix phase of silica material under acidic and alkaline media to develop new composite materials. Zinc oxide is praised for its stability, extended shelf life, and other advantageous qualities, such as wound-healing, astringent, and antibacterial actions. In order to address issues with nanoparticle aggregation, the paper offers a hydrothermal synthesis technique for producing zinc-doped silica. Ultraviolet-visible spectroscopy characterized the synthesized materials by showing the highest absorption around 380 nm, indicating their bandgap energies and optical characteristics. According to scanning electron microscopy examination, alkaline conditions created uniform, well-dispersed granular, spherical morphology, while acidic conditions produced uneven, agglomerated structures. Zn, Si, and O elements were confirmed to be present in both samples by energy-dispersive X-ray spectroscopy spectra, suggesting that the nanocomposite was successfully formed without any observable contaminants. The results highlight the significance of synthesis conditions on the characteristics and possible applications of the synthesized Zn nanoparticles and Zn/Si nanocomposites in ultraviolet optoelectronics, photocatalysis, and wastewater treatment.

Categories: Advanced Materials, Nano Materials, Nanotechnology

Keywords: nanotechnology, inorganic, astringent, antibacterial, optoelectronics

Introduction

One of the most important subfields of materials science is nanotechnology because, in contrast to bulk materials, nanoparticles display novel and enhanced characteristics related to their small size, distribution, and shape [1]. Zinc oxide (ZnO) and zinc-silica (Zn/Si) nanocomposites showed inhibitory effects against selected bacterial and viral models in vitro, which might have been attributed to reactive oxygen species generation and surface interactions; however, their efficacy and safety in vivo had yet to be established [2,3]. Zinc-based nanomaterials, such as metallic zinc (Zn^0) and ZnO, had attracted considerable interest because of their antimicrobial, catalytic, and optical properties [4]. Nevertheless, the phase composition of these materials had a strong influence on their physicochemical behavior since Zn^0 and ZnO exhibited different electronic structures and reactivities. Thus, accurate determination of the synthesized phase was necessary to match the structure with functional performance [5].

How to cite this article:
Chaudhary A, Imtiyaz A, Singh A (October 12, 2026) Development of a Zinc-Based Nanocomposite Embedded in a Silica Matrix and Analysis Using Ultraviolet (UV)-Visible Spectroscopy and Scanning Electron Microscopy. Cureus J Eng 3 : es44388-026-00321-1. DOI https://doi.org/10.7759/s44388-026-00321-1

Zinc nanomaterials had been the subject of intense interest because of their distinct optical, electronic, and catalytic characteristics, which enabled a variety of applications in environmental remediation, sensing, and biomedical fields [6]. Recent studies had attempted to modify Zn by hybridization and composite formation to address its drawbacks, such as rapid electron-hole recombination and low surface reactivity [7]. In this regard, Zn/Si nanocomposites had proven to be promising materials because they possessed an increased surface area, enhanced thermal stability, and improved dispersion of active sites, which collectively enhanced catalytic and biological activities [8,9].

Nevertheless, a significant research gap remained in the development of sustainable and green synthesis methods capable of precisely controlling particle size, morphology, and interfacial interactions in Zn/Si nanocomposites. In addition, little was known about the influence of environmentally friendly synthesis pathways on the multifunctionality, particularly the photocatalytic and biological activities, of these nanocomposites. Therefore, the novelty of the present study lay in the development of a green synthesis strategy for Zn/Si nanocomposites with improved functional performance. This work aimed to synthesize, characterize, and evaluate the structural, optical, and application-oriented properties of Zn/Si nanocomposites, with emphasis on improving photocatalytic and biological activities compared with those of conventional ZnO systems.

As a result, numerous approaches to ZnO nanoparticle synthesis and subsequent surface modification had been proposed to reduce these limitations [10]. Preparing ZnO nanoparticles on inorganic substrates had emerged as an attractive approach. Specifically, Si was a highly versatile material used in various industrial applications and had been proposed as a support for ZnO nanoparticles [11].

A hydrothermal synthesis method offered promising prospects for the effective and sustainable synthesis of Zn-doped Si to overcome these challenges. The method ensured uniform dopant distribution, reduced costs, and saved time by performing both doping and material fabrication in a single step. It also enhanced catalytic activity, reduced waste generation, strengthened dopant-matrix interactions, and provided improved control over morphology. The method could produce a synergistic effect in a simple and economical manner through Si coating and the generation of additional active sites within the siliceous framework without restricting pore accessibility.

The purpose of the present study was to investigate a simple and reproducible synthesis methodology for Zn/Si nanocomposites at different pH values. The novelty of the work was associated with a comparative study of nanocomposites synthesized under acidic and alkaline conditions to evaluate the influence of the chemical environment on composite morphology and optical properties. Unlike studies that focused solely on ZnO, this work examined the potential for Zn-based phase transformations resulting from the synthesis procedures and emphasized the need for careful interpretation of properties arising from the synthesized phases.

This research aimed to (i) synthesize Zn-based nanoparticles and embed them within a Si matrix under controlled acidic and alkaline conditions, (ii) investigate the optical properties of the synthesized materials using ultraviolet (UV)-visible spectroscopy, and (iii) examine the morphology of the synthesized materials using scanning electron microscopy (SEM). The study provided a preliminary understanding of the dependence of the structural and optical properties of Zn/Si nanocomposites on synthesis conditions.

Materials And Methods

Materials

The following materials were used: Zn acetate (Rankem, 99%), silicon dioxide (Loba, 99%), ethanol (Northman, 99.9%), NaOH (Rankem, 98%), and hydrochloric acid (Merck, 35%).

Synthesis of Zn Nanoparticles

Five grams of Zn acetate were dissolved in distilled water, and the solution was stirred for 30 min. After this period, a freshly prepared aqueous $NaBH_4$ solution (0.1 M), added dropwise under continuous stirring, was introduced as a reducing agent. The addition of $NaBH_4$ resulted in the reduction of Zn^{2+} ions and the formation of Zn-containing species.

The reaction mixture was subsequently stirred for an additional 1 h to facilitate particle formation and homogeneous dispersion. Treatment with strong reducing agents such as sodium borohydride ($NaBH_4$) can promote the reduction of Zn^{2+} ions to Zn^0. Under the synthesis conditions, the resulting Zn species may undergo partial oxidation upon exposure to water and dissolved or atmospheric oxygen during processing. However, X-ray diffraction (XRD) analysis revealed a predominantly amorphous structure and did not provide conclusive evidence for the presence of crystalline ZnO or Zn^0 phases.

In aqueous media, the initially formed Zn species may undergo oxidation through hydroxylated intermediate species upon exposure to dissolved oxygen, atmospheric oxygen, and water molecules. Although $NaBH_4$ initially acted as a reducing agent, subsequent oxidation under ambient or thermal conditions may have resulted in the formation of oxidized Zn-containing species. However, the available characterization data, particularly the predominantly amorphous XRD pattern, did not provide conclusive evidence for the formation of crystalline ZnO nanoparticles. Therefore, the synthesized materials are described as Zn-containing nanomaterials, and their structural, optical, and morphological properties were evaluated accordingly. Similar oxidation and phase-transformation processes in borohydride-assisted syntheses of Zn-based materials have been reported previously [12-14].

The obtained product was first dried in a hot-air oven to remove residual moisture and was subsequently calcined in a muffle furnace at 200 °C for 3 h. Finally, the synthesized material was characterized using UV-visible spectroscopy.

Synthesis of Zn/Si Nanocomposite in an Acidic Medium

A hydrothermal method was employed to prepare the Zn/Si nanocomposite under acidic conditions. Briefly, 5.00 g of SiO_2 was added to a 1.0 M HCl solution and magnetically stirred at 500 rpm for 2 h, resulting in the formation of a homogeneous bluish suspension. The synthesized solid was repeatedly washed with deionized (DI) water until a neutral pH (~6-7) was achieved and was subsequently redispersed in 100 mL of DI water and ultrasonicated for 20 min. Previously synthesized Zn nanoparticles were dispersed in the mixture to achieve a 2 wt% Zn loading. The pH was adjusted to 2-3 using 1.0 M HCl while stirring continuously at 500 rpm for an additional 1 h. The resulting suspension was transferred to a Teflon-lined stainless-steel autoclave (filling volume <80% of capacity) and subjected to hydrothermal treatment at 200 °C for 48 h under autogenous pressure of approximately 15-20 bar. After completion of the reaction, the autoclave was cooled to room temperature at a rate of approximately 2-3 °C min^{-1}. The obtained product was centrifuged, washed repeatedly with DI water and ethanol, and dried at 80 °C for 12 h to yield the Zn/Si nanocomposite.

Synthesis of Zn/Si Nanocomposite in an Alkaline Medium

Zinc nanoparticles (2 wt% of the total reaction mixture) were added to the Si suspension and stirred at 600 rpm for 30 min to achieve homogeneous dispersion. Subsequently, a 1.0 M NaOH solution was added dropwise under continuous stirring until the pH reached approximately 10-11. The mixture was then stirred for 1 h at room temperature at 600 rpm to ensure complete homogenization.

The suspension was transferred to a Teflon-lined stainless-steel autoclave (maximum filling level <80%) and subjected to hydrothermal treatment at 200 °C for 48 h. The autogenous pressure inside the autoclave was estimated to be approximately 15-20 bar. After completion of the reaction, the autoclave was cooled to room temperature at a controlled cooling rate of approximately 5 °C h^{-1} and then opened.

The resulting product was centrifuged and washed thoroughly with deionized water and ethanol to remove impurities, followed by drying in a hot-air oven at 80 °C for 12 h. High-temperature calcination was intentionally avoided to prevent uncontrolled oxidation and phase transformation of the Zn-based species. The synthesized nanocomposite was subsequently characterized by UV-visible spectroscopy.

Characterization

XRD patterns were recorded using a PANalytical diffractometer with Cu Kα radiation. Diffraction data were collected over a 2θ range of 10°-80°. UV-visible absorption spectra were measured using a Shimadzu UV-1800 spectrophotometer. Spectral measurements were performed in the wavelength range of 200-800 nm with a resolution of 1 nm. For SEM and

energy-dispersive X-ray spectroscopy (EDX) analyses, the synthesized materials were first deposited as thin films on aluminum foil using a spin-coating process. The samples were then examined using SEM operated at an accelerating voltage of 10 kV. Surface morphology was investigated by acquiring micrographs at various magnifications.

Results And Discussion

UV-visible spectroscopy of synthesized Zn nanoparticles

The UV-visible absorption spectrum of the synthesized Zn nanoparticles was measured over the wavelength range of 200-1,000 nm, and strong absorption was observed in the UV region, followed by a gradual reduction in absorbance within the visible and near-infrared regions, as shown in Figure *1*. The successful synthesis of Zn nanoparticles was confirmed by the presence of a prominent absorption edge in the range of 280-320 nm, which was characteristic of Zn-based nanostructures. This behavior was attributed to strong UV absorption resulting from electronic transitions between the valence and conduction bands, which reflected the intrinsic semiconducting properties of the Zn nanoparticles [15,16].

The absence of distinct peaks in the visible region suggested a relatively homogeneous particle-size distribution and minimal particle aggregation. The smooth decrease in absorbance beyond 400 nm further indicated reduced light scattering and good nanoparticle dispersion. The observed blue-shifted absorption edge of the Zn nanoparticles compared with bulk Zn materials was attributed to quantum confinement effects arising from their nanoscale dimensions. This confinement increased the band-gap energy and enhanced the UV optical response. Furthermore, the weak absorption observed in the visible region suggested a lower density of defects and a lower density of mid-gap electronic states within the synthesized nanoparticles.

How to cite this article:
Chaudhary A, Imtiyaz A, Singh A (October 12, 2026) Development of a Zinc-Based Nanocomposite Embedded in a Silica Matrix and Analysis Using Ultraviolet (UV)-Visible Spectroscopy and Scanning Electron Microscopy. Cureus J Eng 3 : es44388-026-00321-1. DOI https://doi.org/10.7759/s44388-026-00321-1

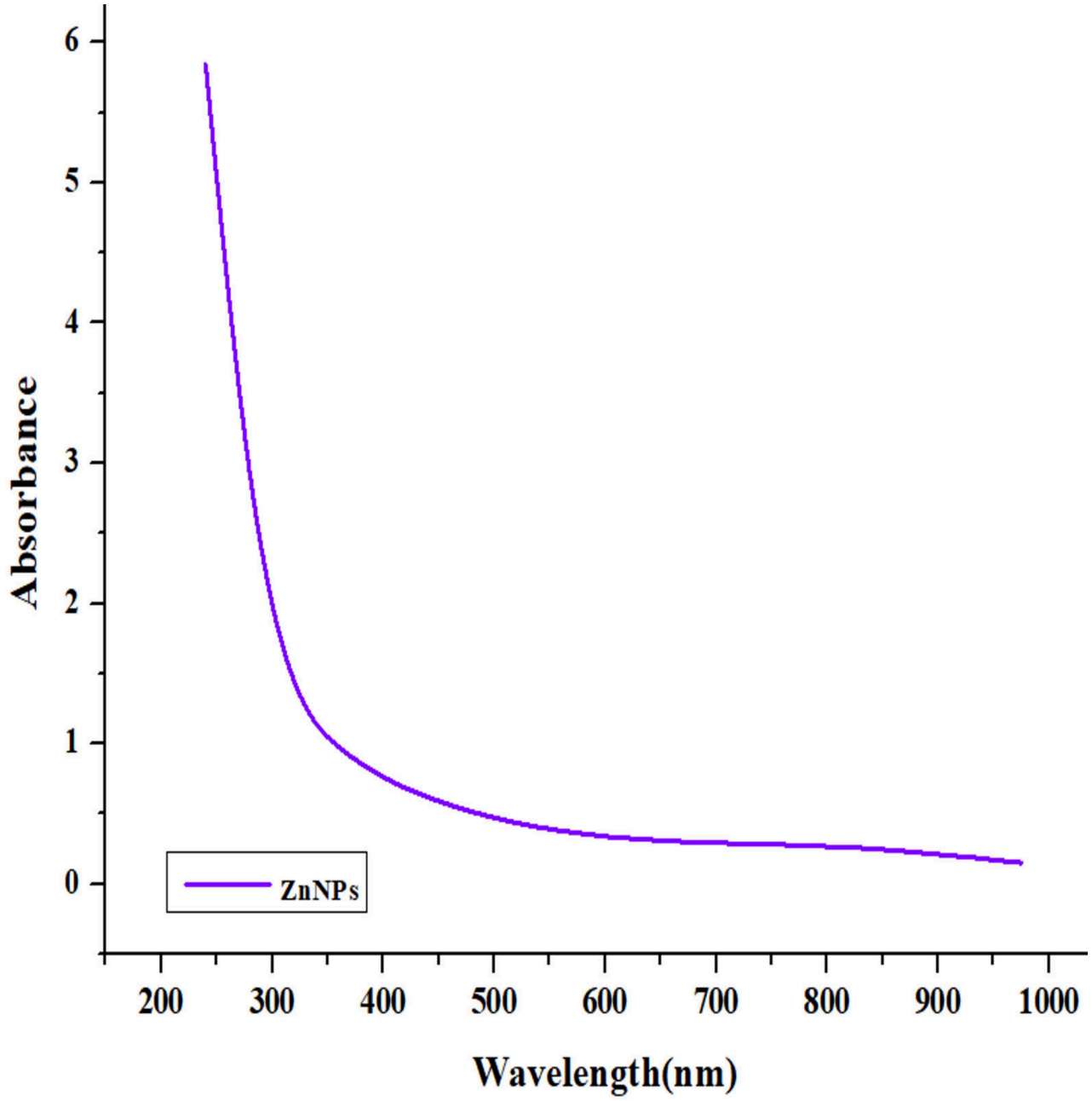


FIGURE 1: UV-visible spectroscopy of synthesized Zn nanoparticles

NPs, Nanoparticles; UV, Ultraviolet

UV-visible spectroscopy was employed to investigate the optical properties of the synthesized Zn nanoparticles, and the Tauc method was utilized to determine the band-gap energy [17]. The absorbance data were used to calculate the absorption coefficient (α), and a Tauc plot was constructed by plotting $(\alpha h\nu)^2$ against photon energy ($h\nu$), assuming a direct allowed electronic transition characteristic of Zn nanoparticles, as shown in Figure *2*.

The optical band gap of the synthesized Zn nanoparticles was calculated from the UV-visible absorption data using the Tauc plot method. The plot of $(\alpha h\nu)^2$ versus photon energy ($h\nu$) exhibited a linear region, which was consistent with the direct allowed electronic transition nature of the material. The linear portion of the curve was extrapolated to the energy axis, and the direct band-gap energy was estimated to be approximately 4.21 eV.

The high band-gap value suggested strong quantum confinement effects and the formation of nanoscale particles within the nanocomposite. The increase in band-gap energy relative to bulk ZnO was attributed to the small particle size and interactions between the Zn species and the Si matrix. The synthesized material exhibited optical properties that could be useful for photocatalytic and optoelectronic applications.

The obtained direct band-gap value (4.21 eV) was considerably higher than the reported values for bulk ZnO (3.2-3.37 eV), which could be attributed to strong interactions between Zn species and the Si matrix, as well as pronounced nanoscale effects. The reduction in crystallite size and the increased number of surface defects were known to increase the band gap of such materials, as reported for other ZnO/SiO_2 nanocomposites. For instance, the band gap of Si-supported ZnO nanocomposites has previously been reported to lie within the range of 3.5-4.0 eV, depending on the synthesis method and particle size.

The higher band-gap value observed in the present study might have resulted from quantum confinement effects, low crystallinity, and the homogeneous dispersion of Zn nanoparticles within the amorphous Si framework. These findings were consistent with previous reports on hydrothermally synthesized Zn-based nanocomposites, which exhibited widened band gaps and enhanced optical properties suitable for photocatalytic applications.

How to cite this article:
Chaudhary A, Imtiyaz A, Singh A (October 12, 2026) Development of a Zinc-Based Nanocomposite Embedded in a Silica Matrix and Analysis Using Ultraviolet (UV)-Visible Spectroscopy and Scanning Electron Microscopy. Cureus J Eng 3 : es44388-026-00321-1. DOI https://doi.org/10.7759/s44388-026-00321-1

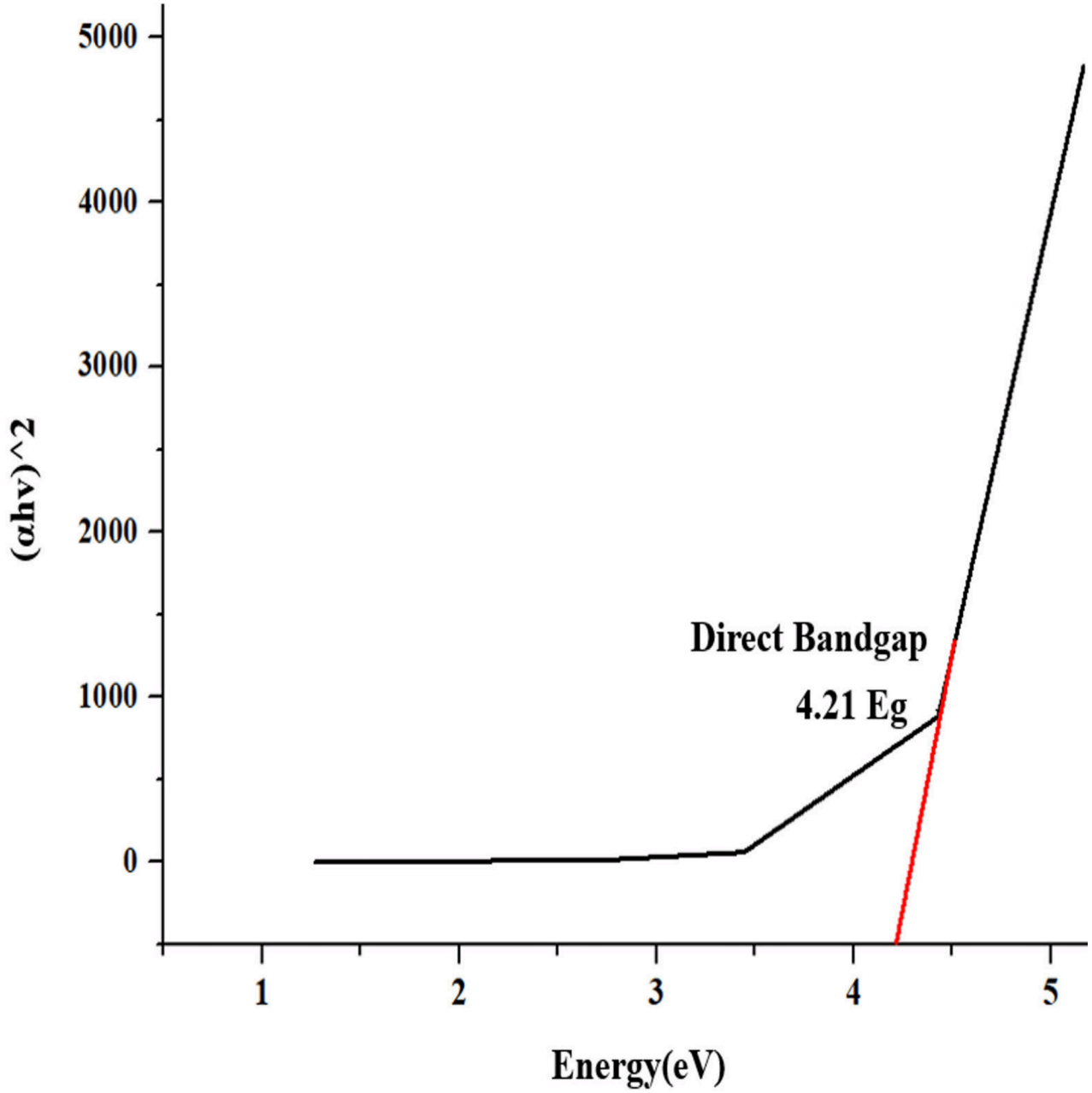


FIGURE 2: Band gap representation of synthesized Zn nanoparticles

UV-visible spectroscopy of the synthesized Zn/Si nanocomposite in an acidic medium

Figure *3* displayed the UV-visible absorption spectrum of the synthesized Zn/Si nanocomposite recorded in the wavelength range of 300-1,000 nm. A strong absorption band was observed in the UV region below approximately 380 nm, which was characteristic of Zn-based materials and was attributed to the intrinsic band-to-band electronic transition from the valence band to the conduction band. The pronounced absorption in the UV region confirmed the successful formation of Zn-based nanoparticles within the SiO_2 matrix. SiO_2, being an optically transparent and insulating material, did not contribute additional strong absorption peaks but influenced the optical behavior by modifying the electronic environment of the Zn species. In addition, a broad and weak absorption band was observed extending into the visible

region (400-800 nm) [18]. This behavior was attributed to interfacial interactions between Zn species and SiO_2, surface oxygen vacancies, or defect states within the nanocomposite. Such defect-related absorption was known to enhance the light-harvesting capability and had frequently been reported in nanocomposite systems.

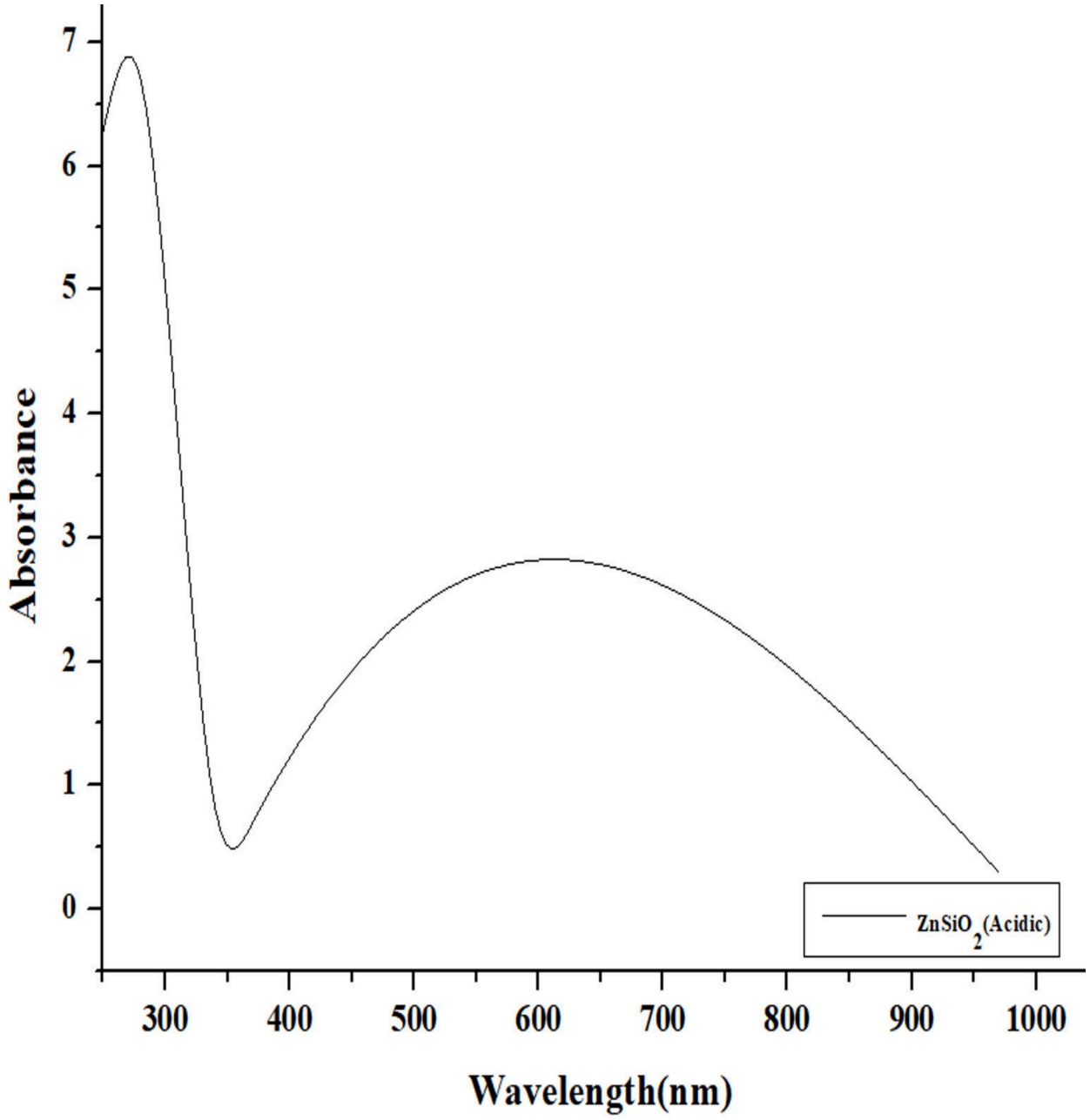


FIGURE 3: UV-visible spectroscopy of the synthesized Zn/Si nanocomposite in an acidic medium

UV, Ultraviolet

Band-gap analysis of the synthesized Zn-SiO_2 nanocomposite in an acidic medium

UV-visible spectroscopy was employed to investigate the optical properties of the synthesized Zn-SiO_2 nanocomposite, and the Tauc method was utilized to determine the band-gap energy. The absorbance data were used to calculate the absorption coefficient (α), and a Tauc plot was constructed by plotting $(\alpha h\nu)^2$ against photon energy ($h\nu$), assuming a

direct allowed electronic transition characteristic of Zn-based materials, as shown in Figure *4*.

The optical band gap of the synthesized Zn/Si nanocomposite prepared in an acidic medium was determined using the Tauc plot obtained from UV-visible spectroscopy. The linear relationship observed in the $(\alpha h\nu)^2$ versus photon energy ($h\nu$) plot confirmed the direct allowed transition nature of the material. By extrapolating the linear portion of the curve to the energy axis, the direct band-gap energy was estimated to be 3.56 eV.

The obtained band-gap value was higher than that of bulk ZnO (3.2-3.37 eV), which could be attributed to nanoscale particle formation, quantum confinement effects, and interactions between Zn species and the amorphous Si matrix [19]. Compared with previously reported ZnO/SiO_2 nanocomposites, where band-gap values generally ranged from 3.4 to 4.0 eV depending on synthesis conditions and particle size, the present result fell within the reported range.

A similar enhancement in band-gap energy had been observed in hydrothermally synthesized Si-supported ZnO nanocomposites due to reduced crystallinity and improved particle dispersion. The comparatively moderate band-gap value obtained in the acidic medium suggested better crystallinity than that of an alkaline sample while still maintaining nanoscale optical characteristics favorable for photocatalytic applications.

How to cite this article:
Chaudhary A, Imtiyaz A, Singh A (October 12, 2026) Development of a Zinc-Based Nanocomposite Embedded in a Silica Matrix and Analysis Using Ultraviolet (UV)-Visible Spectroscopy and Scanning Electron Microscopy. Cureus J Eng 3 : es44388-026-00321-1. DOI https://doi.org/10.7759/s44388-026-00321-1

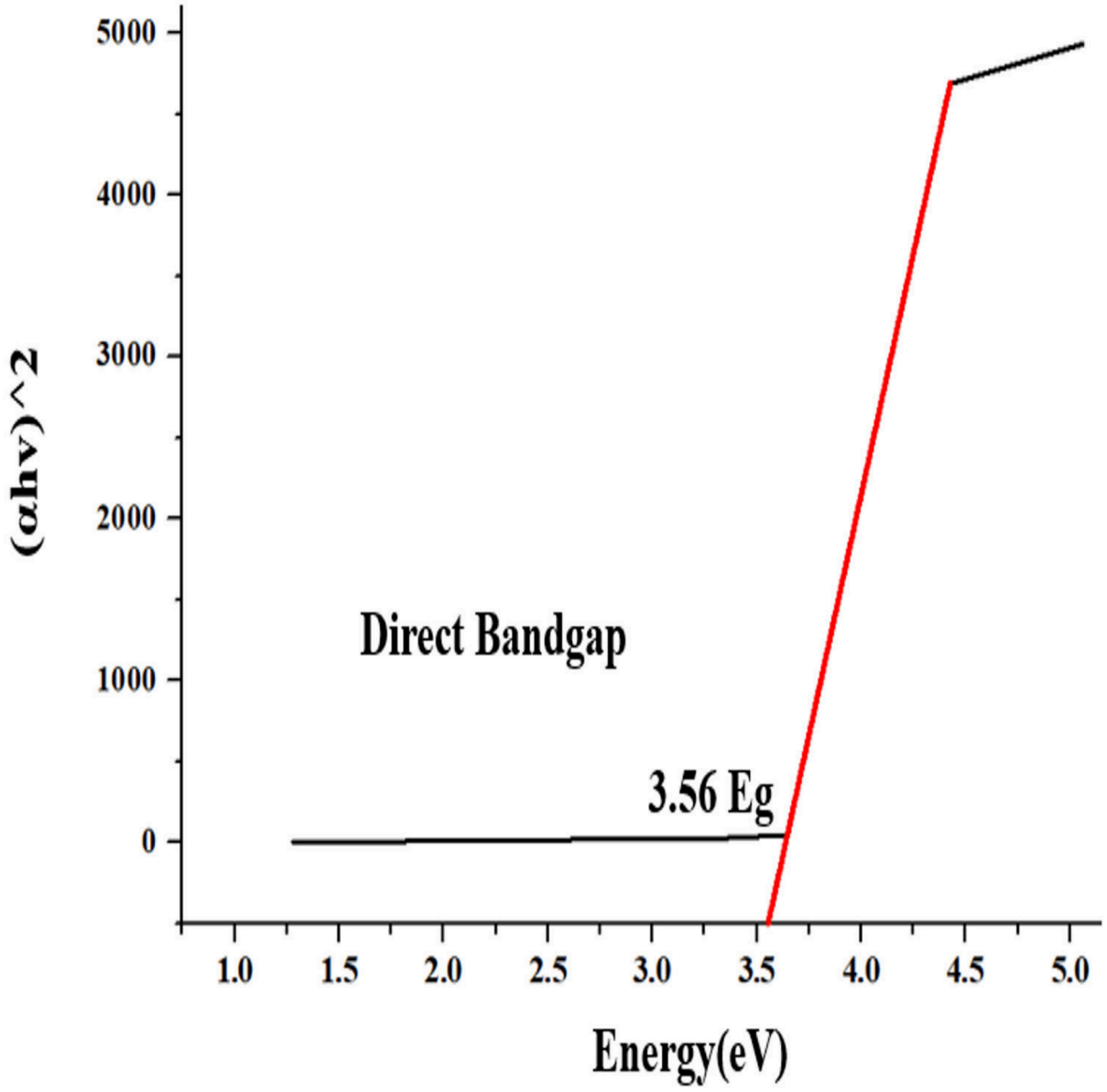


FIGURE 4: Band gap representation of the synthesized Zn/Si nanocomposite in an acidic medium

SEM and EDX analysis of the synthesized Zn/Si nanocomposite in an acidic medium

The SEM micrograph revealed an agglomerated and uneven surface morphology with particles that were not uniformly dispersed, as shown in Figure *5*. Smaller granular domains and larger plate-like fractured structures were observed, suggesting partial aggregation and surface erosion induced by the acidic environment. The acidic medium promoted particle coalescence and structural distortion, possibly due to enhanced surface protonation and dissolution-reprecipitation processes. These morphological characteristics indicated reduced dispersion and increased clustering of nanoparticles under acidic conditions, which could have influenced their surface reactivity and functional performance.

The particle-size distribution histogram, together with the Gaussian fitting curve, indicated that the nanoparticles were predominantly distributed within the range of 20-60 nm, with a maximum frequency occurring between 30 and 50 nm, as shown in Figure *6*.

The fitted Gaussian curve suggested a moderately narrow particle-size distribution, confirming the formation of nanoscale particles with a certain degree of polydispersity. This behavior was consistent with the SEM observations, where smaller primary nanoparticles appeared to form agglomerated structures.

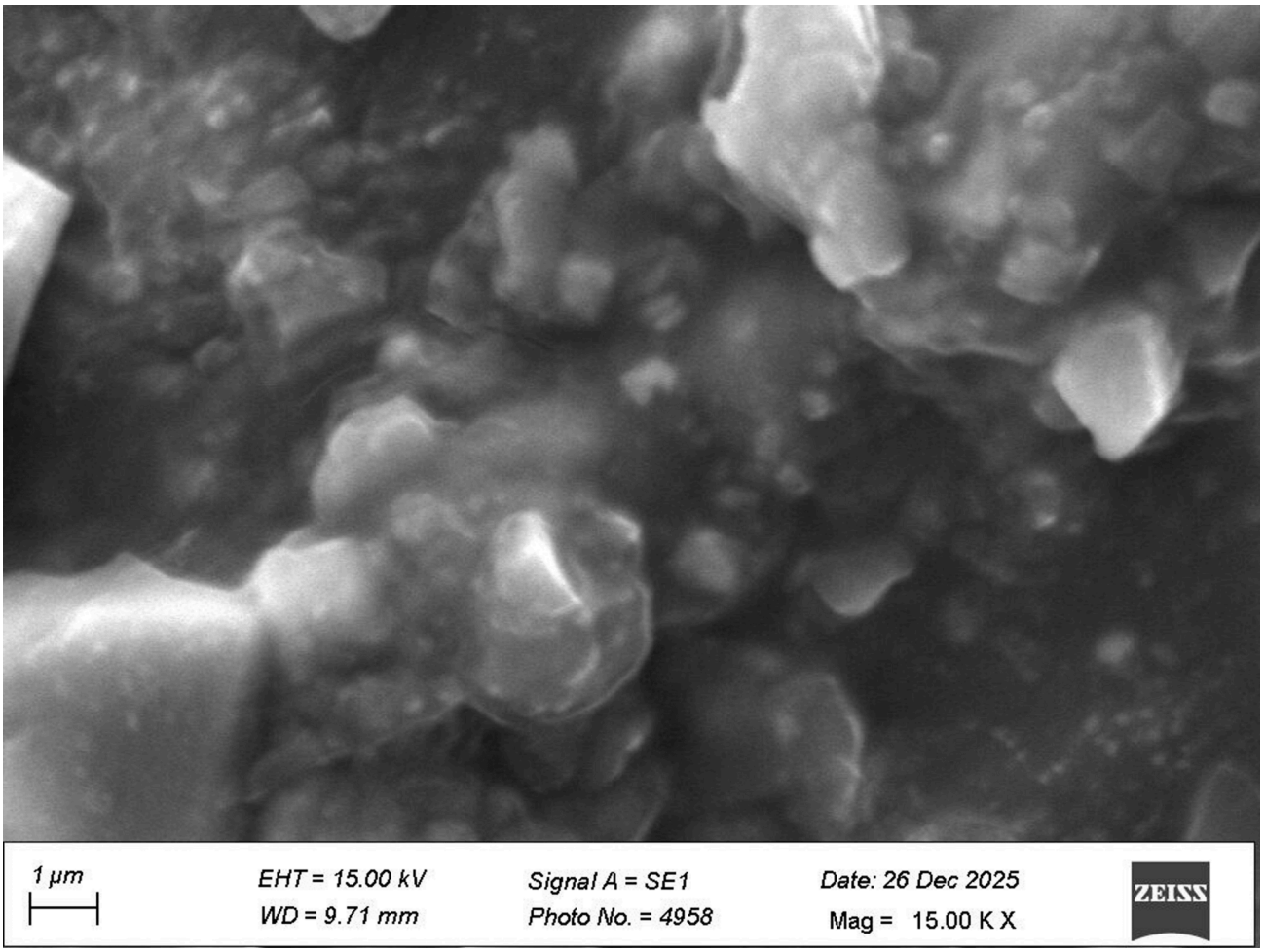


FIGURE 5: SEM analysis of the synthesized Zn/Si nanocomposite in an acidic medium

EHT, Electron High Tension; SEM, Scanning Electron Microscopy; WD, Working Distance

How to cite this article:
Chaudhary A, Imtiyaz A, Singh A (October 12, 2026) Development of a Zinc-Based Nanocomposite Embedded in a Silica Matrix and Analysis Using Ultraviolet (UV)-Visible Spectroscopy and Scanning Electron Microscopy. Cureus J Eng 3 : es44388-026-00321-1. DOI https://doi.org/10.7759/s44388-026-00321-1

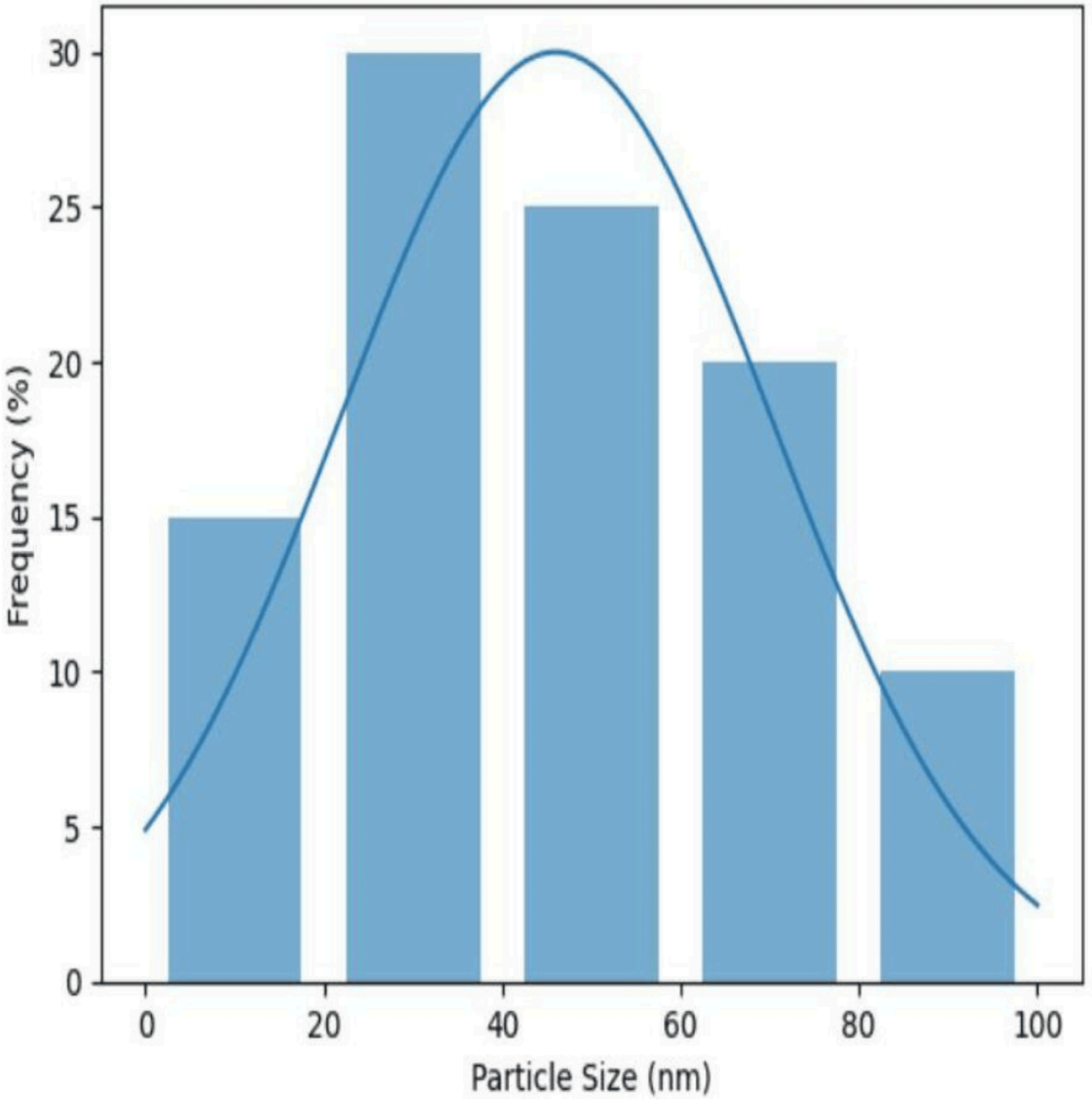


FIGURE 6: Histogram analysis of the synthesized Zn/Si nanocomposite in an acidic medium

EDX analysis of the Zn-SiO_2 nanocomposite in an acidic medium

The successful formation of the Zn-Si nanocomposite in an acidic medium was confirmed by the EDX spectrum. Prominent peaks corresponding to Zn (Zn L and Zn K lines), Si (Si Kα), and O (O Kα) were observed, indicating that Zn, Si, and oxygen were the principal constituents of the composite, as shown in Figure *7*. The oxygen peak originated from both the Si matrix and the Zn-based oxide species present in the material.

The absence of any significant impurity peaks suggested the high purity of the synthesized nanocomposite. The elemental composition was consistent with the aggregated morphology observed in the SEM analysis under acidic conditions and confirmed the successful incorporation of Zn species within the Si framework. Furthermore, the presence

How to cite this article:
Chaudhary A, Imtiyaz A, Singh A (October 12, 2026) Development of a Zinc-Based Nanocomposite Embedded in a Silica Matrix and Analysis Using Ultraviolet (UV)-Visible Spectroscopy and Scanning Electron Microscopy. Cureus J Eng 3 : es44388-026-00321-1. DOI https://doi.org/10.7759/s44388-026-00321-1

of distinct Zn, Si, and O peaks in the EDX spectrum demonstrated that the Zn-Si nanocomposite had been successfully synthesized without any detectable contaminants.

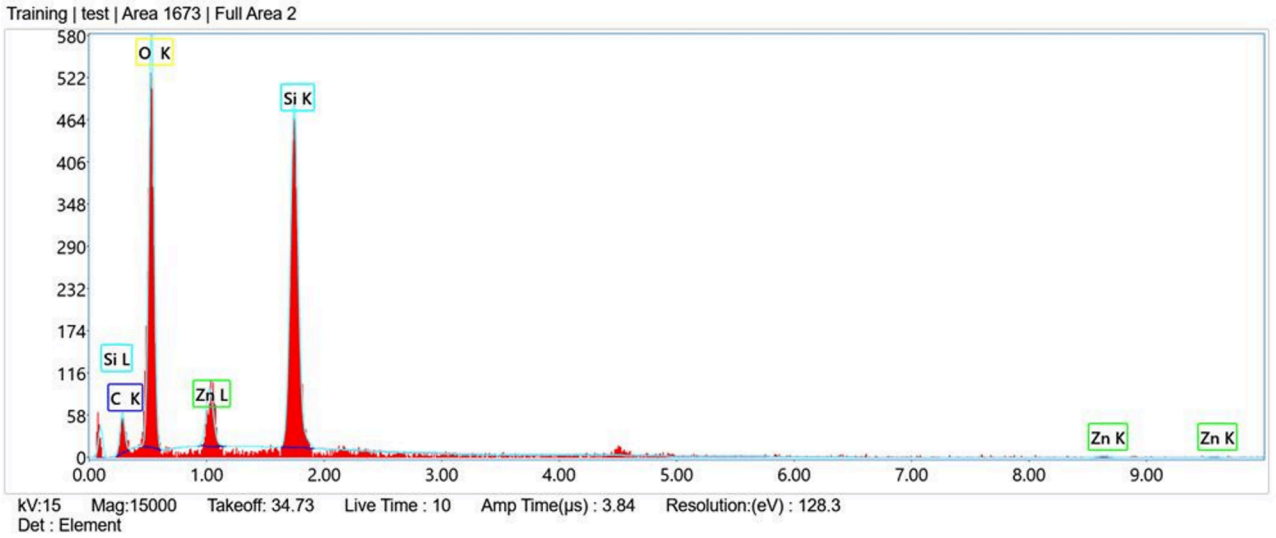


FIGURE 7: EDX analysis of the synthesized Zn/Si nanocomposite in an acidic medium

EDX, Energy-Dispersive X-ray Spectroscopy

XRD analysis of the synthesized Zn/Si nanocomposite in an acidic medium

The XRD pattern of the Zn/Si nanocomposite showed a broad diffraction hump in the range of 22-28°, which was characteristic of a highly amorphous Si matrix, as shown in Figure *8*. The absence of sharp and intense diffraction peaks indicated the low crystallinity of the material and the nanoscale dimensions of the particles. The broad peak centered at $2\theta \approx 24°$ was attributed to amorphous SiO_2, a phase commonly observed in Si-based materials synthesized through green or chemical routes.

The diffuse background and the presence of weak diffraction peaks around 31°, 34°, and 36° were assigned to characteristic planes of Zn-containing phases, which could be indexed to the crystal planes of hexagonal ZnO. However, the intensities of these peaks were very low, and the peaks were considerably broadened, suggesting that the Zn species were highly dispersed within the Si matrix and possessed very small crystallite sizes.

The reduced peak intensity further validated the successful incorporation of Zn nanoparticles into the SiO_2 framework without significant agglomeration. The gradual decrease in intensity at higher diffraction angles also confirmed that the synthesized Zn/Si material was nanostructured and partially amorphous. The presence of plant-derived phytochemicals during the synthesis process likely contributed to the broad diffraction profile observed in the green-synthesized metal-Si nanocomposite, as these phytochemicals were known to regulate crystal growth during nanoparticle formation.

Overall, the XRD analysis confirmed the formation of an amorphous Zn/Si nanocomposite consisting of a Si matrix with highly dispersed ZnO nanoparticles. The material exhibited structural characteristics associated with a high surface area, making it potentially suitable for catalytic, photocatalytic, and antimicrobial applications.

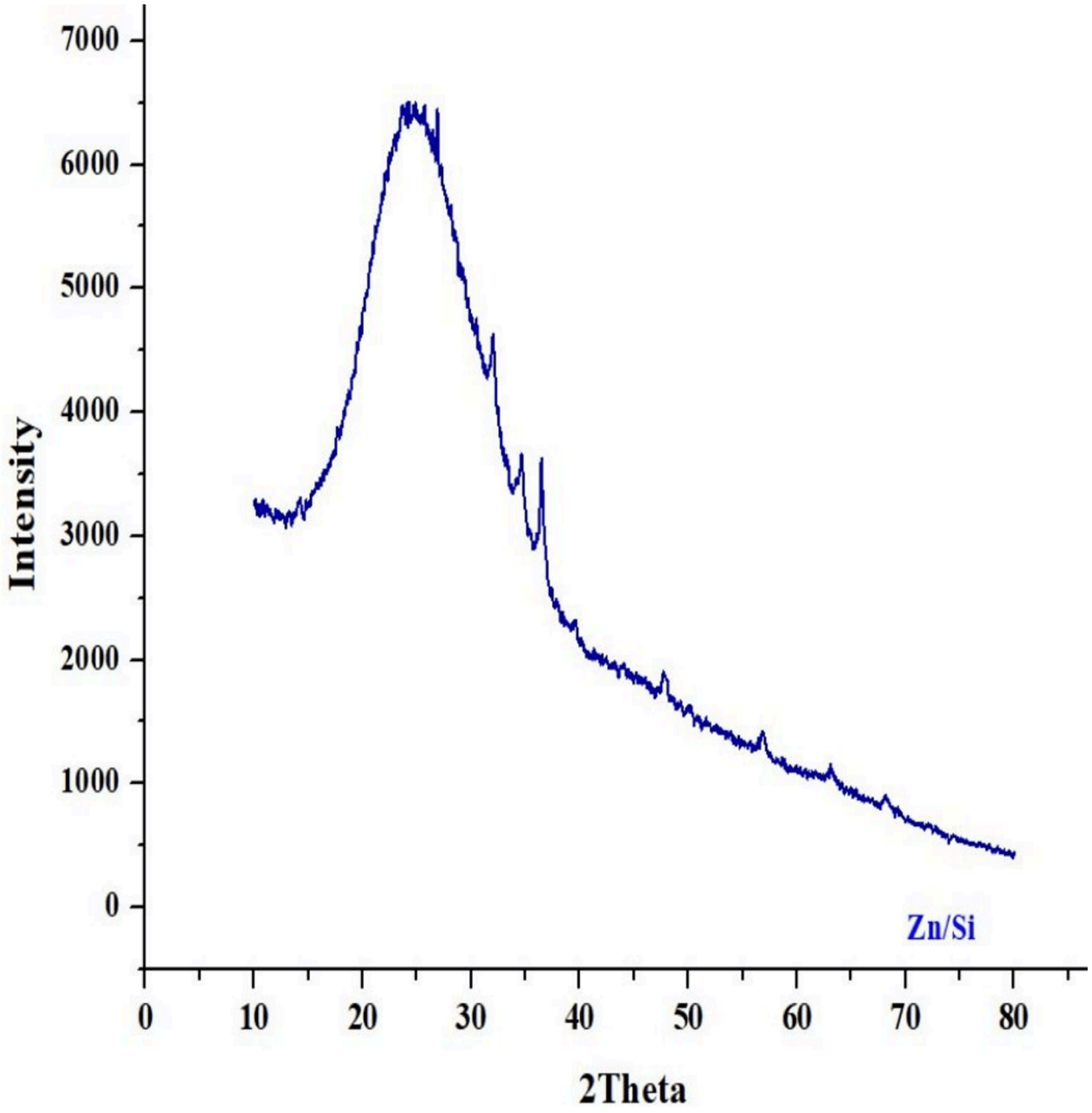


FIGURE 8: XRD analysis of the synthesized Zn/Si nanocomposite in an acidic medium

XRD, X-Ray Diffraction

Figure *9* displayed the UV-visible absorption spectrum of the Zn-SiO_2 nanocomposite synthesized under alkaline conditions, recorded over the wavelength range of 200-1,000 nm. Significant absorption was observed in the UV region below approximately 400 nm, which was attributed to the intrinsic band-to-band transition of Zn-based species resulting from electron excitation from the valence band to the conduction band.

A broad absorption tail extending into the visible region (400-800 nm) was also observed. This behavior was attributed to oxygen vacancies, Zn interstitials, and surface defect states generated during synthesis under alkaline conditions. Furthermore, localized energy states within the band gap were believed to arise from interfacial interactions between the Zn species and the SiO_2 matrix.

The reduced absorbance intensity observed at longer wavelengths (>800 nm) confirmed the semiconducting nature of the nanocomposite and suggested the absence of metallic impurities. Overall, the spectral behavior indicated that the alkaline-synthesized Zn-SiO_2 nanocomposite possessed enhanced optical absorption and a modified band structure, which could be advantageous for photocatalytic and optoelectronic applications [20].

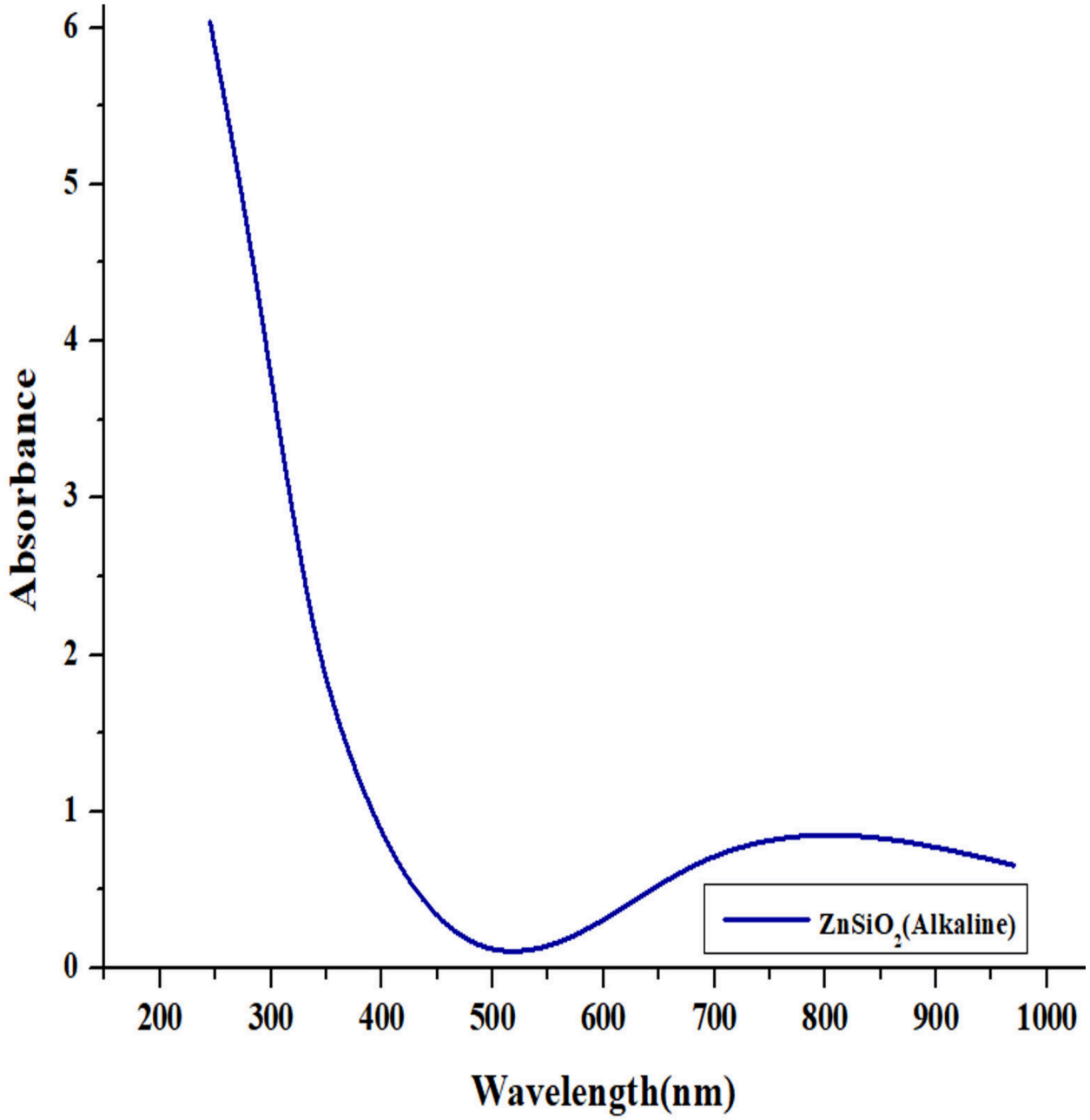


FIGURE 9: UV-visible spectroscopy of the synthesized Zn/Si nanocomposite in an alkaline medium

UV, Ultraviolet

Band gap analysis of the Zn-SiO_2 nanocomposite synthesized in an alkaline medium

UV-visible spectroscopy was employed to investigate the optical properties of the synthesized Zn-SiO_2 nanocomposite, and the Tauc method was utilized to determine the band-gap energy. The absorbance data were used to calculate the absorption coefficient (α), and a Tauc plot was constructed by plotting $(\alpha h\nu)^2$ against photon energy ($h\nu$), assuming a direct allowed electronic transition characteristic of Zn-based materials [21], as shown in Figure *10*.

A distinct linear region was observed near the absorption edge in the Tauc plot, and extrapolation of this region yielded a direct band-gap energy of approximately 3.31 eV. The obtained band-gap value confirmed the direct band-gap nature of the nanocomposite and was found to be close to that reported for bulk ZnO.

The alkaline-synthesized sample exhibited a slightly lower band-gap value than the acidic-synthesized sample, which could be attributed to improved crystallinity, larger particle size, and stronger interactions between the Zn species and the SiO_2 matrix under alkaline conditions. The observed narrowing of the band gap might also have resulted from the introduction of localized electronic states near the band edges by surface defects and oxygen vacancies generated during alkaline synthesis.

How to cite this article:
Chaudhary A, Imtiyaz A, Singh A (October 12, 2026) Development of a Zinc-Based Nanocomposite Embedded in a Silica Matrix and Analysis Using Ultraviolet (UV)-Visible Spectroscopy and Scanning Electron Microscopy. Cureus J Eng 3 : es44388-026-00321-1. DOI https://doi.org/10.7759/s44388-026-00321-1

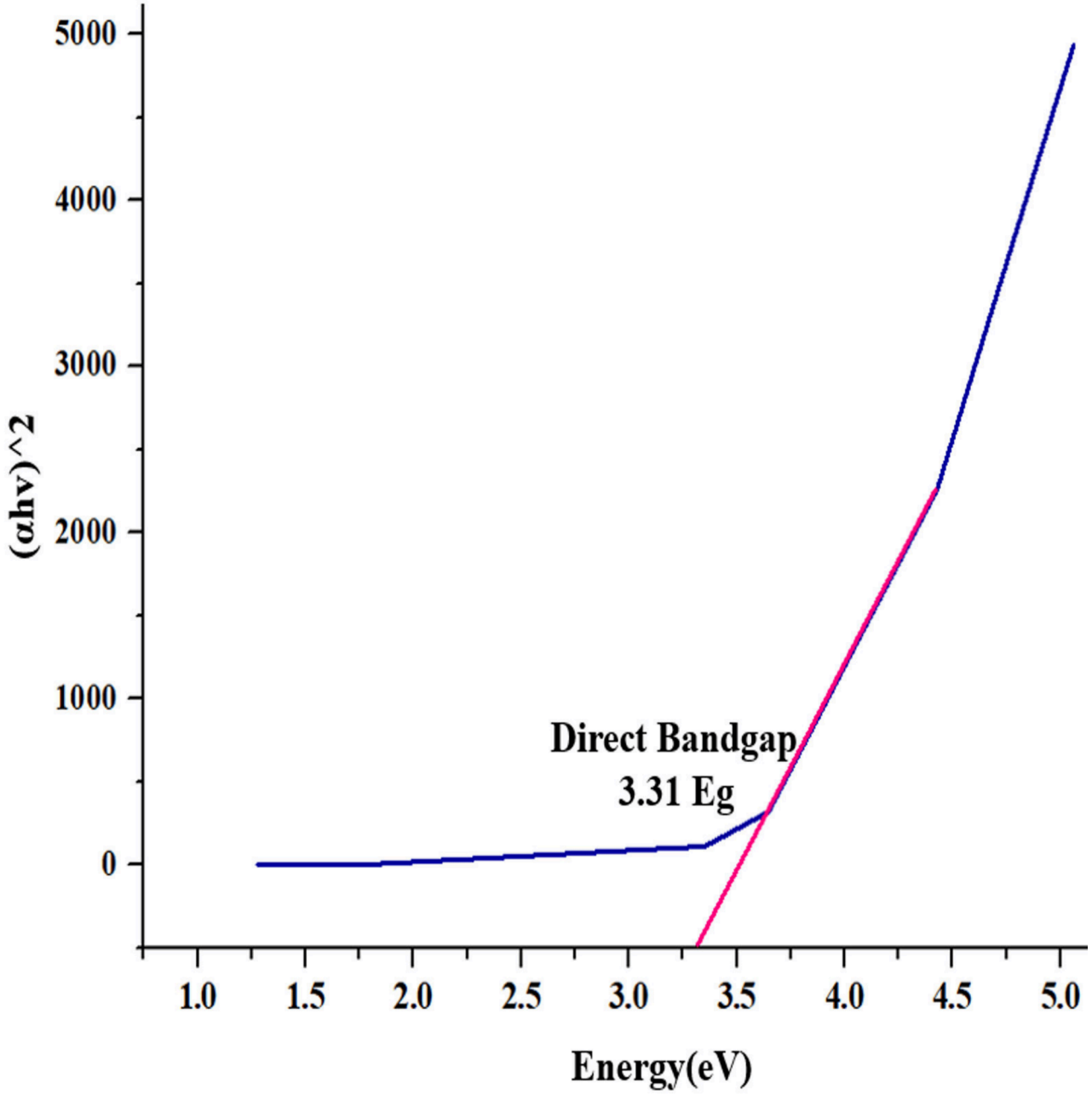


FIGURE 10: Band gap representation of the synthesized Zn/Si nanocomposite in an alkaline medium

SEM analysis of the synthesized Zn/Si nanocomposite in an alkaline medium

In the alkaline medium, SEM analysis revealed a relatively homogeneous, finely dispersed, and densely packed morphology, as shown in Figure *11*. In contrast to the acidic medium, the nanocomposite consisted of quasi-spherical to irregular granular particles that were distributed across the surface with reduced aggregation. The presence of smaller particle domains and improved surface uniformity suggested that alkaline conditions favored the controlled nucleation and growth of Zn-based nanoparticles within the Si matrix.

How to cite this article:
Chaudhary A, Imtiyaz A, Singh A (October 12, 2026) Development of a Zinc-Based Nanocomposite Embedded in a Silica Matrix and Analysis Using Ultraviolet (UV)-Visible Spectroscopy and Scanning Electron Microscopy. Cureus J Eng 3 : es44388-026-00321-1. DOI https://doi.org/10.7759/s44388-026-00321-1

The enhanced dispersion observed under alkaline conditions was attributed to improved surface-charge stabilization, which prevented excessive particle coalescence. This morphology provided a higher effective surface area, which was advantageous for catalytic activity and optical absorption.

The particle-size distribution histogram (Figure *12*) indicated that the synthesized nanoparticles possessed a relatively narrow size distribution in the range of 20-60 nm, with the maximum frequency occurring between 20 and 40 nm. The average particle size was calculated to be approximately 45 nm, with a standard deviation of approximately 20 nm, indicating moderate polydispersity. Furthermore, the distribution followed an approximately Gaussian profile, as demonstrated by the fitted curve, suggesting uniform nucleation and growth behavior during synthesis. The observed size range was consistent with the morphological features obtained from SEM analysis, although a certain degree of particle aggregation was also observed.

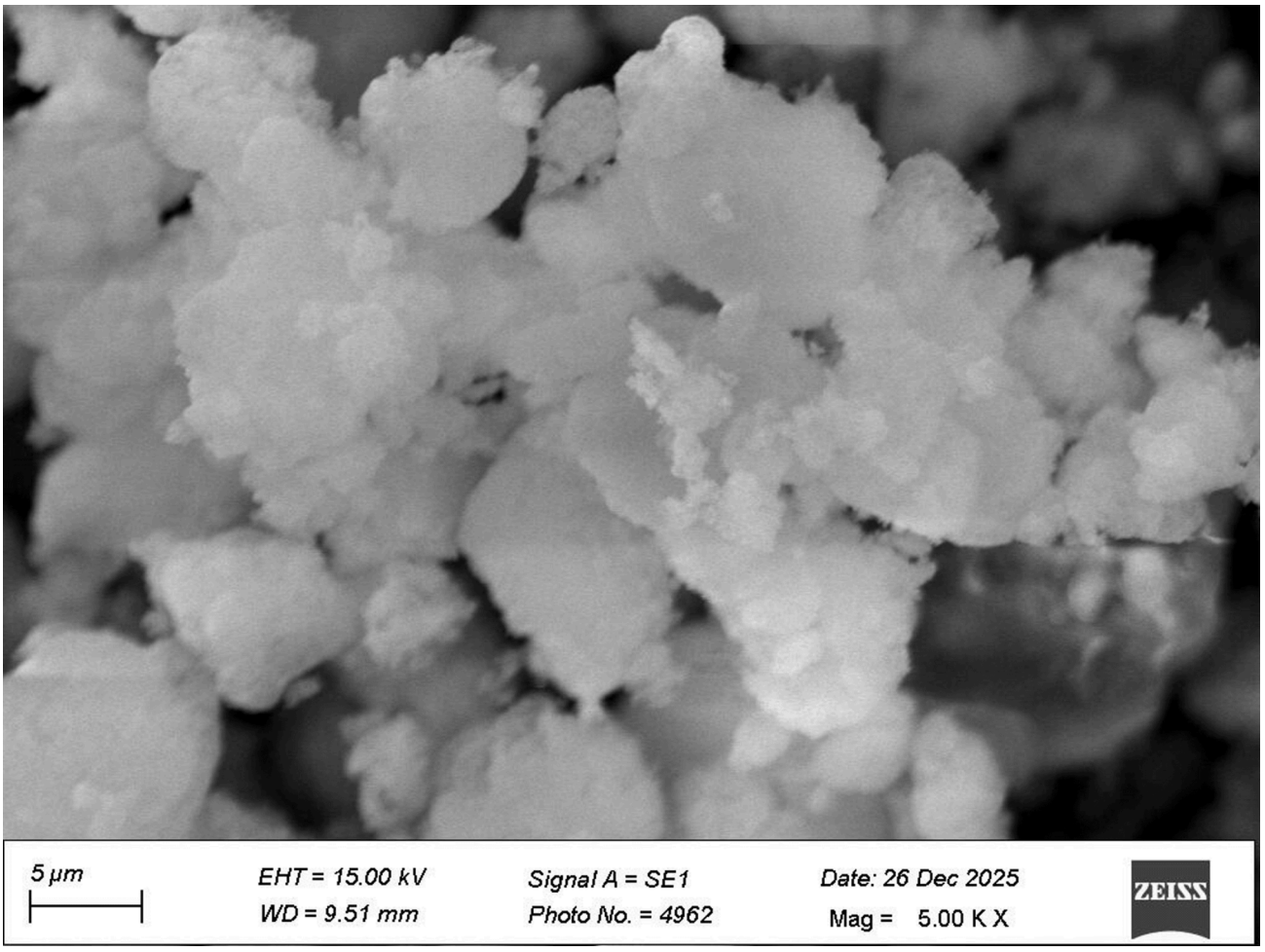


FIGURE 11: SEM analysis of the synthesized Zn/Si nanocomposite in an alkaline medium

SEM, Scanning Electron Microscopy

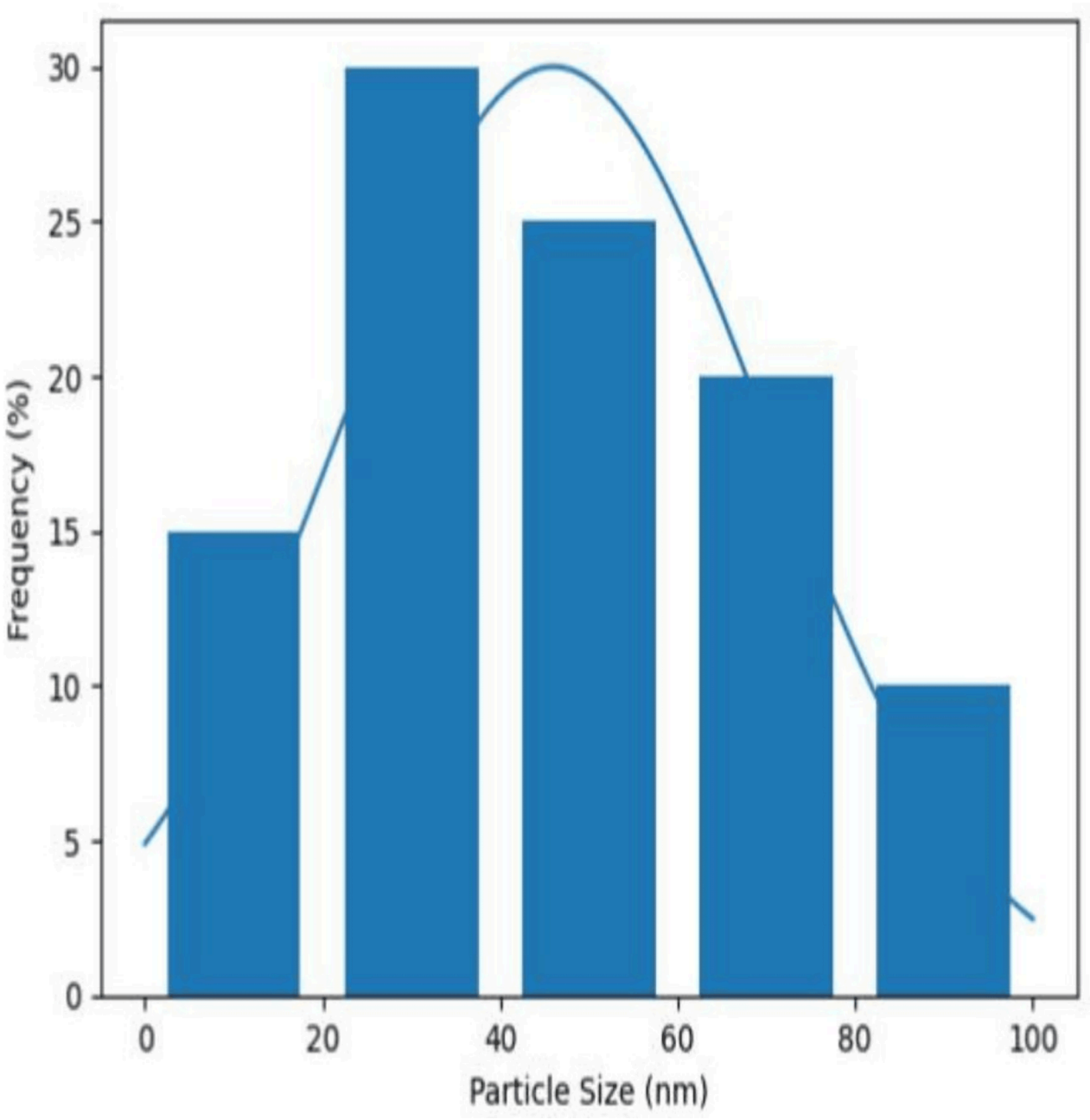


FIGURE 12: Histogram analysis of the synthesized Zn/Si nanocomposite in an alkaline medium

The elemental composition of the Zn-Si nanocomposite synthesized in an alkaline medium was verified by the EDX spectrum. The successful incorporation of Zn species within the Si matrix was confirmed by the clear presence of distinct peaks corresponding to Zn (Zn L and Zn K lines), Si (Si Kα), and O (O Kα), as shown in Figure *13*. The alkaline-synthesized sample exhibited comparatively sharper and more intense Zn and Si peaks than the sample prepared in acidic medium, indicating improved elemental distribution and greater compositional uniformity. The oxygen signal originated from both the ZnO and SiO_2 phases present in the nanocomposite.

The absence of additional peaks associated with contaminants indicated the high purity of the synthesized material. Furthermore, the uniform morphology observed in the SEM analysis was consistent with the enhanced elemental homogeneity achieved under alkaline conditions.

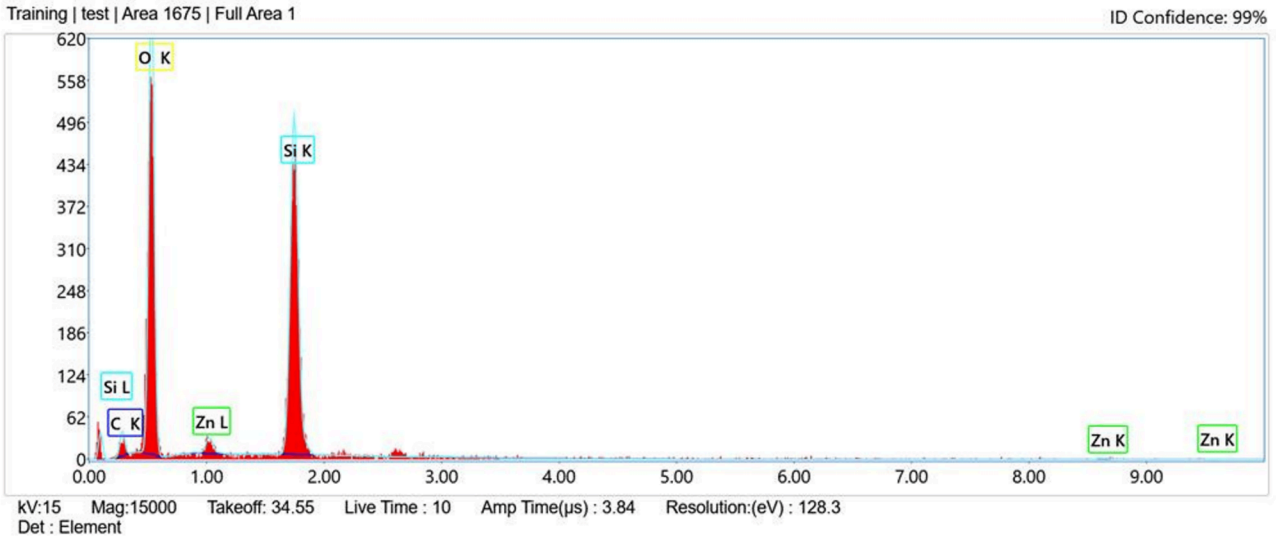


FIGURE 13: EDX analysis of the synthesized Zn/Si nanocomposite in an alkaline medium

EDX, Energy-Dispersive X-ray Spectroscopy

XRD analysis of the synthesized Zn/Si nanocomposite in an alkaline medium

The XRD pattern of the synthesized Zn/Si nanocomposite prepared in alkaline medium showed a broad and intense diffraction peak at a 2θ value of approximately 22-25°, which was characteristic of amorphous Si (SiO_2), as shown in Figure *14*. The broad peak suggested a non-crystalline or poorly crystalline structure of the Si matrix. The absence of sharp diffraction peaks further indicated that the material was predominantly amorphous and possessed nanoscale structural features.

The weak diffraction features observed in the region of 30-35° could be attributed to ZnO-related crystal planes; however, their low intensity suggested that the ZnO particles were either extremely small in size or highly dispersed within the amorphous Si network. This phenomenon had previously been reported for Si-supported ZnO nanocomposites synthesized using green and wet-chemical methods.

Furthermore, the absence of distinct reflections and the gradual decrease in diffraction intensity from 35° to 80° demonstrated that the amorphous phase predominated, thereby confirming the formation of a homogeneous Zn/Si nanocomposite. The reduced crystallinity could have been advantageous for catalytic and photocatalytic applications because amorphous materials generally possessed a higher density of surface defects and a larger active surface area, resulting in enhanced adsorption capacity and reactivity.

In conclusion, the XRD analysis confirmed that the alkaline synthesis route successfully produced a Zn/Si nanocomposite with a predominantly amorphous structure, finely dispersed Zn species, and nanoscale structural characteristics suitable for environmental, catalytic, and photocatalytic applications.

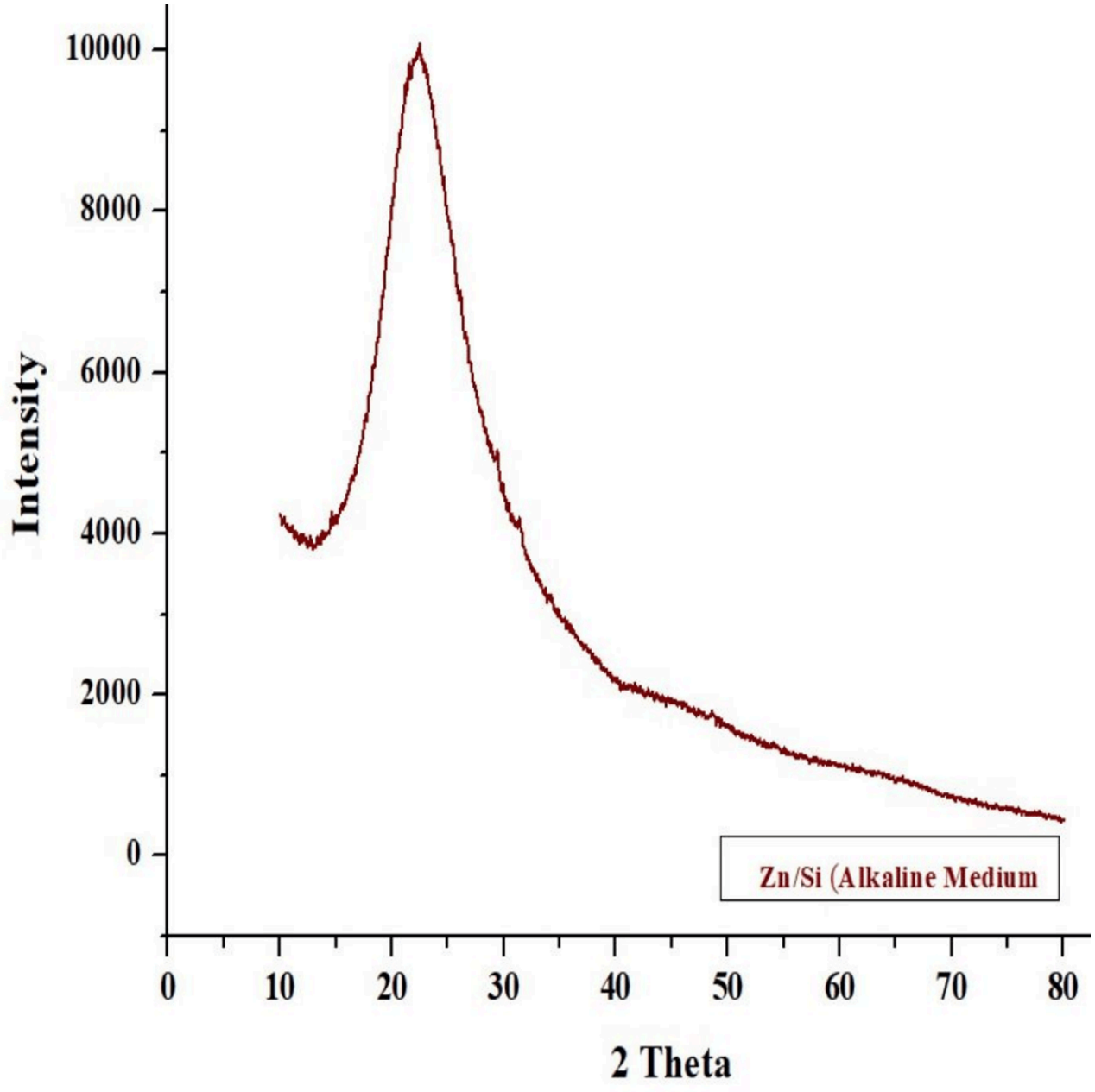


FIGURE 14: XRD analysis of the synthesized Zn/Si nanocomposite in an alkaline medium

XRD, X-Ray Diffraction

Comparative UV-visible, optical band gap, SEM, and EDX analysis

The optical behavior of Zn nanoparticles and Zn-SiO_2 nanocomposites synthesized in acidic and alkaline media differed significantly, as evidenced by the UV-visible absorption spectra and corresponding Tauc plots, confirming the substantial influence of composition and synthesis environment on the electronic structure, as shown in Table *1*. Zn nanoparticles exhibited strong absorption in the UV region below approximately 350 nm, followed by a gradual decrease in absorbance across the visible and near-infrared regions. This behavior was characteristic of nanoscale Zn-based systems and indicated interband electronic transitions with minimal visible-light absorption, suggesting a relatively low defect density.

In contrast, the Zn-SiO_2 nanocomposite synthesized in acidic medium exhibited a broader absorption profile extending well into the visible region (400-800 nm) [22]. The increased absorbance and spectral broadening were attributed to enhanced light-matter interactions resulting from the presence of SiO_2, which modified the local electronic environment and generated interfacial states between the Zn species and the Si matrix.

The Zn-SiO_2 nanocomposite synthesized under alkaline conditions exhibited comparatively smoother absorption characteristics, accompanied by a noticeable red shift and an extended absorption tail toward longer wavelengths. This behavior suggested improved crystallinity, stronger interfacial coupling, and enhanced particle dispersion under alkaline conditions, which resulted in modified optical transitions.

A comparative SEM-EDX analysis further demonstrated that the synthesis medium significantly influenced the morphology and elemental distribution of the Zn-Si nanocomposite. SEM micrographs of the sample synthesized in acidic medium revealed uneven, agglomerated, and partially fractured structures, indicating uncontrolled particle growth and surface instability. Correspondingly, the EDX spectrum confirmed the presence of Zn, Si, and O; however, comparatively broader and less intense peaks suggested non-uniform elemental distribution and localized clustering of Zn species within the Si matrix.

In contrast, the alkaline-synthesized sample exhibited a more homogeneous and densely packed morphology, characterized by finer granular features and reduced agglomeration. The corresponding EDX spectrum displayed sharper and more intense Zn and Si peaks, indicating improved compositional uniformity and more effective incorporation of Zn species into the SiO_2 framework.

In both samples, the oxygen signal originated from the Zn and SiO_2 phases; however, the alkaline medium promoted enhanced surface-charge stabilization, resulting in improved particle dispersion and structural stability. Overall, the combined SEM-EDX results demonstrated that acidic conditions tended to promote aggregation and compositional heterogeneity, whereas alkaline synthesis conditions favored controlled nucleation, homogeneous elemental distribution, and morphological stability. These differences were expected to significantly influence the optical, catalytic, and photocatalytic performance of the synthesized nanocomposites.

How to cite this article:
Chaudhary A, Imtiyaz A, Singh A (October 12, 2026) Development of a Zinc-Based Nanocomposite Embedded in a Silica Matrix and Analysis Using Ultraviolet (UV)-Visible Spectroscopy and Scanning Electron Microscopy. Cureus J Eng 3 : es44388-026-00321-1. DOI https://doi.org/10.7759/s44388-026-00321-1

S. No.	Properties	Zn NPs	Zn/SiO_2 (Acidic)	Zn/SiO_2 (Alkaline)
1	Band Gap	4.21 eV	3.56 eV	3.31 eV
2	Transition Type	Direct allowed	Direct allowed	Direct allowed
3	Quantum Confinement	Strong	Moderate	Low
4	Visible-Light Activity	Low	Medium	High
5	Defect Influence	Minimal	Higher	Reduced
6	Absorption Region (nm)	200-350 (Strong UV absorption), 350-1,000 (Gradual decrease)	250-400 (Intense absorption), 400-800 (Moderate absorption)	250-380 (Smooth absorption), 400-900 (Extended tail)
7	Band Gap Trend	Highest Eg	Reduced Eg	Lowest Eg
8	Application Suitability	UV optoelectronics	UV-visible photocatalysis	Visible-light photocatalysis, wastewater treatment
9	Key Observation	Strong quantum confinement, the smallest particle size	Band gap narrowing due to interfacial states	Further band gap reduction, improved electronic coupling

TABLE 1: Comparative table for UV-visible analysis of Zn NPs, Zn/SiO_2 (acidic), and Zn/SiO_2 (alkaline)

NPs, Nanoparticles; UV, Ultraviolet

Conclusions

In this study, Zn-containing nanoparticles and Zn/Si nanocomposites were synthesized in acidic and alkaline media via a hydrothermal route, and their structural, optical, and morphological characteristics were investigated. UV-visible spectroscopy and Tauc plot analysis revealed strong absorption in the UV region and direct band-gap behavior, indicating that the synthesis medium significantly influenced the optical properties of the obtained materials. Morphological analysis demonstrated that samples synthesized in acidic medium exhibited relatively agglomerated structures, whereas alkaline conditions promoted improved particle dispersion and a more homogeneous distribution of Zn species within the Si matrix. SEM and EDX analyses confirmed the presence and distribution of Zn and Si elements in the synthesized nanocomposites. XRD patterns indicated the predominantly amorphous nature of the Si support and suggested the presence of highly dispersed nanoscale Zn-containing species, although no highly crystalline Zn-based phase was detected.

The observed differences in morphology, elemental distribution, and optical properties demonstrate that the synthesis environment plays an important role in determining the characteristics of Zn/Si nanocomposites. These results provide insight into the influence of pH on the formation and dispersion of Zn species within Si matrices and contribute to the

development of Si-supported Zn-based nanomaterials. Further investigations involving advanced phase characterization and application-specific performance studies are required to establish the relationship between structure and functional properties.

Additional Information

Author Contributions

All authors have reviewed the final version to be published and agreed to be accountable for all aspects of the work.

Concept and design: Ajay Singh, Aakarsh Chaudhary

Acquisition, analysis, or interpretation of data: Ajay Singh, Aakarsh Chaudhary, Asima Imtiyaz

Critical review of the manuscript for important intellectual content: Ajay Singh, Aakarsh Chaudhary

Supervision: Ajay Singh

Drafting of the manuscript: Asima Imtiyaz

Disclosures

Human subjects: All authors have confirmed that this study did not involve human participants or tissue.

Animal subjects: All authors have confirmed that this study did not involve animal subjects or tissue.

Conflicts of interest: In compliance with the ICMJE uniform disclosure form, all authors declare the following:

- **Payment/services info:** All authors have declared that no financial support was received from any organization for the submitted work.
- **Financial relationships:** All authors have declared that they have no financial relationships at present or within the previous three years with any organizations that might have an interest in the submitted work.
- **Other relationships:** All authors have declared that there are no other relationships or activities that could appear to have influenced the submitted work.

Data Availability Statements

The datasets (and/or code) supporting this study are available from the corresponding author upon reasonable request.

References

1. Dizaj SM, Lotfipour F, Barzegar-Jalali M, Zarrintan MH, Adibkia K: Antimicrobial activity of the metals and metal oxide nanoparticles. Materials Science and Engineering: C. 2014, 44:278-284. 10.1016/j.msec.2014.08.031
2. Nocchetti M, Donnadio A, Ambrogi V, Andreani P, Bastianini M, Pietrella D, Latterini L: Ag/AgCl nanoparticle decorated layered double hydroxides: synthesis, characterization and antimicrobial properties. Journal of Materials Chemistry B. 2013, 1:2383-2393. 10.1039/c3tb00561e
3. Ambrogi V, Donnadio A, Pietrella D, et al.: Chitosan films containing mesoporous SBA-15 supported silver nanoparticles for wound dressing. Journal of Materials Chemistry B. 2014, 2:6054-6063. 10.1039/c4tb00927d
4. Jawale V, Gugale G, Chaskar M, et al.: Two- and three-dimensional zinc oxide nanostructures and its photocatalytic dye degradation performance study. Journal of Materials Research. 2021, 36:1573-1583. 10.1557/s43578-021-00174-w
5. Jawale V, Al-fahdawi A, Salve S, et al.: 6, 13-pentacenequinone/zinc oxide nanocomposites for organic dye degradation. Materials Today: Proceedings. 2022, 52:17-20. 10.1016/j.matpr.2021.10.098

How to cite this article:
Chaudhary A, Imtiyaz A, Singh A (October 12, 2026) Development of a Zinc-Based Nanocomposite Embedded in a Silica Matrix and Analysis Using Ultraviolet (UV)-Visible Spectroscopy and Scanning Electron Microscopy. Cureus J Eng 3 : es44388-026-00321-1. DOI https://doi.org/10.7759/s44388-026-00321-1

6. Zaware AA, Jawale VS, Mehere AC, et al.: Rietveld-refined structural modulation of Zn-substituted Ni Fe_2 O_4 nanostructures for enhanced photocatalytic performance. Polyhedron. 2026, 291:118078. 10.1016/j.poly.2026.118078
7. Shinde CS, Sali ND, Dhawale SK, Dhanwate VN, Jawale V: Influence of Co2+ ions on structural, optical, and magnetic properties of inverse spinel lithium ferrite nanoparticles. Cureus Journal of Engineering. 2025, 1-14. 10.7759/s44388-024-02854-9
8. Zhao X, Han Y, Zhu T, et al.: Electrospun polylactide-nano-hydroxyapatitevancomycin composite scaffolds for advanced osteomyelitis therapy. Journal of Biomedical Nanotechnology. 2019, 15:1213-1222. 10.1166/jbn.2019.2773
9. Smijs TG, Pavel S: Titanium dioxide and zinc oxide nanoparticles in sunscreens: focus on their safety and effectiveness. Nanotechnology, Science and Applications. 2011, 4:95-112. 10.2147/nsa.s19419
10. Schwartz JR, Marsh RG, Draelos ZD: Zinc and skin health: overview of physiology and pharmacology. Dermatologic Surgery. 2005, 31:837-847. 10.1111/j.1524-4725.2005.31729
11. Singh A, Singh NB, Afzal S, Singh T, Hussain I: Zinc oxide nanoparticles: a review of their biological synthesis, antimicrobial activity, uptake, translocation and biotransformation in plants. Journal of Materials Science. 2018, 53:185-201. 10.1007/s10853-017-1544-1
12. Cao G, Wang Y: Nanostructures and Nanomaterials: Synthesis, Properties, and Applications. World Scientific Publishing, Singapore; 2011.
13. Kołodziejczak-Radzimska A, Jesionowski T: Zinc oxide—from synthesis to application: a review. Materials. 2014 , 7:2833-2881. 10.3390/ma7042833
14. Baruah S, Dutta J: Hydrothermal growth of ZnO nanostructures. Science and Technology of Advanced Materials. 2009, 10:013001. 10.1088/1468-6996/10/1/013001
15. Yao W, Wang Y, Wang X, Zhu J, Zhang Z, Yuan X: CuInS2 thin films obtained by solid-state sulfurization. Materials Science in Semiconductor Processing. 2014, 26:175-181. 10.1016/j.mssp.2014.04.021
16. Becheri A, Dürr M, Lo Nostro P, Baglioni P: Synthesis and characterization of zinc oxide nanoparticles: application to textiles as UV-absorbers. Journal of Nanoparticle Research. 2008, 10:679-689. 10.1007/s11051-007-9318-3
17. Tauc J, Grigorovici R, Vancu A: Optical properties and electronic structure of amorphous germanium. Physica Status Solidi (B). 1966, 15:627-637. 10.1002/pssb.19660150224
18. Yao LQ, Chen GH, Yang T, Cui SC, Li ZC, Yang Y: Energy transfer, tunable emission and optical thermometry in Tb3+/Eu3+ co-doped transparent NaCaPO4 glass ceramics. Ceramics International. 2016, 42:13086-13090. 10.1016/j.ceramint.2016.05.092
19. Dhawale SK, Sarvalkar PD, Shinde CS, Prasad NR, Garadkar KM, Sharma KKK, Ramteke AA: Studies on photocatalytic and antioxidant efficacy of Ag-embedded ZnO nanocomposites. ACS Omega. 2025, 10:11948-11960. 10.1021/acsomega.4c08896
20. Du L, Du W, Zhao Y, et al.: Ternary nickel-cobalt selenide nanosheet arrays with enhanced electrochemical performance for hybrid supercapacitors. Journal of Alloys and Compounds. 2019, 778:848-857. 10.1016/j.jallcom.2018.11.105
21. Cai H, Chen X, Li Q, He B, Tang Q: Enhanced photocatalytic activity from Gd, La codoped TiO2 nanotube array photocatalysts under visible-light irradiation. Applied Surface Science. 2013, 284:837-842. 10.1016/j.apsusc.2013.08.018
22. Li K, Haneda M, Gu Z, Wang H, Ozawa M: Modification of CeO2 on the redox property of Fe2O3. Materials Letters. 2013, 93:129-132. 10.1016/j.matlet.2012.09.039

How to cite this article:
Chaudhary A, Imtiyaz A, Singh A (October 12, 2026) Development of a Zinc-Based Nanocomposite Embedded in a Silica Matrix and Analysis Using Ultraviolet (UV)-Visible Spectroscopy and Scanning Electron Microscopy. Cureus J Eng 3 : es44388-026-00321-1. DOI https://doi.org/10.7759/s44388-026-00321-1